



# Computational screening and design of traditional Chinese medicine (TCM) to block phosphodiesterase-5

Calvin Yu-Chian Chen <sup>a,b,\*</sup>

<sup>a</sup> Laboratory of Pharmacoinformatics and Nanotechnology, School of Chinese Medicine, China Medical University, Taichung, 40402, Taiwan, ROC

<sup>b</sup> Department of Bioinformatics, Asia University, Taichung, 41354, Taiwan, ROC

## ARTICLE INFO

### Article history:

Received 9 April 2009

Received in revised form 31 July 2009

Accepted 3 August 2009

Available online 8 August 2009

### Keywords:

Phosphodiesterase-5 (PDE-5)

Traditional Chinese medicines (TCM)

Erectile dysfunction

Multiple linear regressions (MLR)

Pharmacophore analysis

## ABSTRACT

The traditional Chinese medicines (TCM), *Epimedium sagittatum* (ESs), *Cnidium monnieri* (CMs), and *Semen cuscutae* (SCs), were used for treating erectile dysfunction since the ancient Han dynasty (202 BC–AD 220). Phosphodiesterase-5 (PDE-5) is deemed the target protein for inhibition to treat erectile dysfunction. In this study, a reliable multiple linear regression (MLR) model ( $r$  value = 0.8484) was used to predict the activities of new candidates which were designed from ES, CM, and SC. From docking and pharmacophore analysis, the potent candidates among ES, CM, and SC were screened. SC01, SC03, and ES03b were predicted to have high potencies based on MLR analysis and high docking scores. Additionally, from our analysis, we make the follow conclusion (1) Hydrophobic compounds tend to be more potent PDE-5 inhibitors; (2) Because of the big binding site, inhibitors with molecular weights over 500 remain potent; (3) From the pharmacophore analysis, the features of hydrogen bond acceptors are the basis for designing novel inhibitors of PDE-5 and (4) According to MLR analysis, the number of ring groups could be up to 6, but the number of aromatic rings was limited to 4 to be potent. This study offers an alternative way to screen PDE-5 inhibitors from TCM and provides a scientific basis for confirming pharmacological actions of TCM.

© 2009 Elsevier Inc. All rights reserved.

## 1. Introduction

*Epimedium sagittatum* (ESs), *Cnidium monnieri* (CMs), and *Semen cuscutae* (SCs) have been used for treating erectile dysfunction since ancient Chinese era [1–4]. However, their biological mechanisms of actions remain unclear. The major compounds of ESs, CMs, and SCs have been analyzed and are listed in Tables 1–3, respectively. The aim of this work is to study the interaction between these major components and phosphodiesterase-5 (PDE-5).

Penile erection is a physiological response resulting in smooth muscle relaxation and inflow of blood to the corpus cavernosum. It is mediated by releasing the neurotransmitter nitric oxide (NO) from both nitrergic nerves and sinusoidal endothelium. NO activates soluble guanylyl cyclase in cavernosal smooth muscle, resulting in increased synthesis of cyclic GMP (cGMP) and subsequent relaxation of smooth muscle. The concentration of cGMP in the corpus cavernosum is regulated by soluble guanylyl cyclase and cyclic nucleotide phosphodiesterases (PDEs) [5,6]. PDE-5 is an enzyme responsible for degrading cGMP. High concentration of cGMP decreases the intracellular level of calcium

ions in vascular smooth muscle cells of the penis, which leads to erection. The well known inhibitors of PDE-5, such as sildenafil citrate (Viagra) and tadalafil (Cialis), are widely used for treating erectile dysfunction [7,8]. However, the side effects of taking sildenafil citrate and tadalafil were headache and optical dysfunction caused by the inhibitory effects on PDE-6 and PDE-11 [8–10].

From previous studies [11–14], application of both the receptor-based and the ligand-based approaches improved the reliability in molecular simulation. In addition to receptor-based docking study, ligand-based multiple linear regression was also used in this study [15–18]. Combination of receptor-based and ligand-based methods to improve reliability of, a large number of putative inhibitors of PDE-5 were screened [19–21].

The flow chart of the experimental design in this study is shown in Fig. 1.

## 2. Methodology

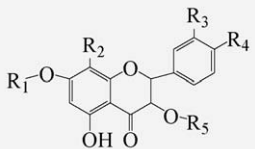
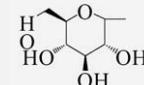
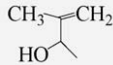
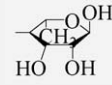
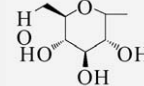
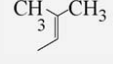
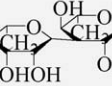
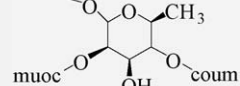
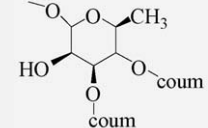
### 2.1. Dataset

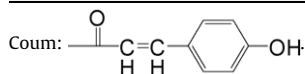
All the molecular simulations were performed by Discovery Studio modeling 2.1 (Accelrys Inc., San Diego, USA). Three-dimensional (3D) molecule model of PDE-5-sildenafil citrate complex was obtained from Protein Data Bank website (PDB ID:

\* Current address: Department of Computational and Systems Biology, Massachusetts Institute of Technology, Cambridge, MA 02139, USA.

E-mail addresses: [ycc@mail.cmu.edu.tw](mailto:ycc@mail.cmu.edu.tw), [ycc0929@mit.edu](mailto:ycc0929@mit.edu).

**Table 1**The components of *Epimedium sagittatum*.

Name	Scaffold	R1	R2	R3	R4	R5
ES01				H	OMe	
ES02				OH	OMe	
ES03a		H	H	H	OH	
ES03b		H	H	H	OH	



1UDT) [22]. Major components of the ESs (Table 1), CMs (Table 2), and SCs (Table 3) were drawn by ChemDraw Ultra 10.0 (Cambridgesoft Inc., USA) and transformed to 3D molecule models by Chem3D Ultra 10.0 (Cambridgesoft Inc., USA). All the simulations were also applied by the forcefield of the Chemistry at Harvard Macromolecular mechanics (CHARMm) which uses a flexible and comprehensive empirical energy function, a summation of many individual energy terms, to perform the prediction. CHARMm is estimated based on separable internal coordinate terms and pairwise nonbond interaction terms [23]. The total energy was calculated by the following equation:

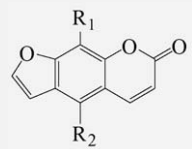
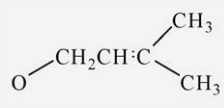
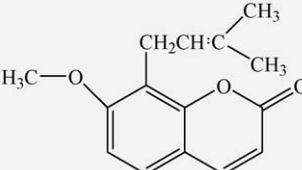
$$E_{\text{pot}} = E_{\text{bond}} + E_{\text{angle}} + E_{\text{torsion}} + E_{\text{oop}} + E_{\text{elec}} + E_{\text{vdw}} + E_{\text{constraint}} + E_{\text{user}} \quad (1)$$

The out-of-plane (OOP) angle was defined as an improper torsion [23]. After all the molecular simulations, hydrogen molecules were fitted in and partial charges of molecules were estimated and assigned.

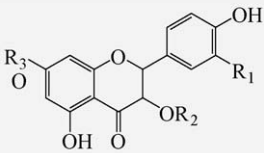
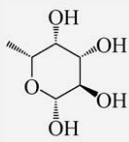
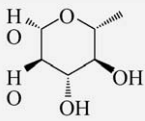
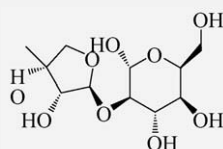
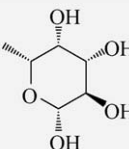
## 2.2. MLR analysis

I employed the compounds from Xia's study [24] to build the MLR model. The properties of molecules in the training set including AlogP, molecular energy, molecular weight (MW), molecular solubility (MS), number of rotatable bonds (NRB), number of rings (NR), number of aromatic rings (NAR), number of hydrogen bond acceptors (NHA), number of hydrogen bond donors (NHD), and molecular polar surface area (PSA) were calculated by

**Table 2**The components of *Cnidium monnieri*.

Name	Scaffold	R1	R2
CM01		OCH <sub>3</sub>	H
CM02		OCH <sub>3</sub>	OCH <sub>3</sub>
CM03		H	OCH <sub>3</sub>
CM04		H	
CM05			

**Table 3**The components of *Semen cuscudae*.

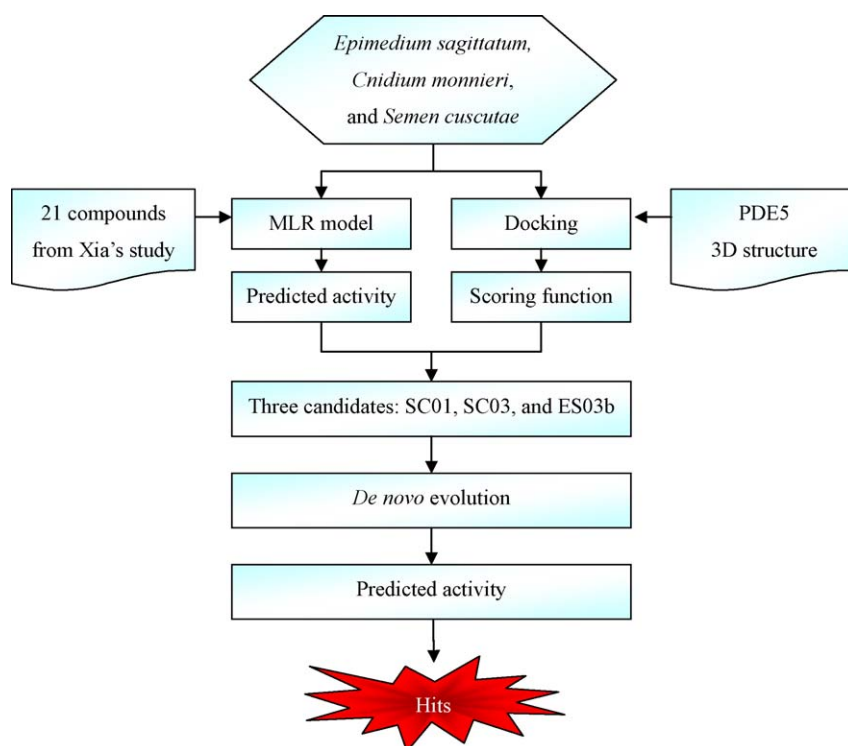
Name	Scaffold	R1	R2	R3
SC01		OH		
SC02		OH		H
SC03		OH		H
SC04		OH	H	H
SC05		H	H	H

Discovery Studio modeling 2.1 (Accelrys Inc., San Diego, USA). The QSAR model was built by multiple linear regressions and was used to characterize the pharmaceutical activities in this study [25–28].

### 2.3. Docking and scoring analysis

Docking scores of ligands with PDE-5 were calculated by Accelrys Discovery studio V2.1 using the forcefield of CHARMM.

The complex of PDE-5 with cGMP, sildenafil citrate, and tadalafil were set up for calculating their docking scores as control groups. In this study, the maximum pose was set to be 10, RMS threshold for diversity was 1.5, and score threshold for diversity was 20.0. The algorithm of the minimization energy tolerance was at zero and the gradient tolerance was 0.001 by default. The docking scores of the major components from ESs, CMs, and SCs with PDE5, as well as control groups, were calculated by the same protocol as referred to above.

**Fig. 1.** The flow chart of the experimental designing in this study.

**Table 4**

The MLR and QSAR models.

Name	MW	Alog P	Energy	MS	NR	NHA	NAR	PSA	MLRT empModel	Predicted activity
Sildenafil citrate	389.404	2.183	70.44	−3.288	6	4	3	74.87	7.794	7.989
ES02	692.661	0.741	181.42	−3.539	5	14	2	254.51	6.375	6.315
ES03a	724.663	5.369	84.38	−7.657	6	12	4	218.73	9.319	9.787
ES03b	724.663	5.369	102.43	−7.68	6	12	4	218.73	9.526	10.031
CM01	760.647	−3.606	102.94	−0.427	6	21	2	344.67	22.431	25.249
CM02	466.392	−0.268	27.61	−1.349	4	12	2	206.59	7.155	7.235
CM03	466.392	−0.268	27.61	−1.349	4	12	2	206.59	7.155	7.235
CM04	288.252	1.721	18.61	−1.951	3	6	2	107.21	1.199	0.211
CM05	628.533	−2.197	47.59	−1.342	5	17	2	285.74	16.056	17.731
SC01	244.286	3.74	47.23	−3.974	2	3	1	35.53	13.145	14.298
SC02	216.19	2.186	35.38	−3.047	3	3	2	48.67	7.336	7.448
SC03	246.215	2.17	48.16	−3.054	3	4	2	57.9	10.705	11.421
SC04	216.19	2.186	45.54	−3.055	3	3	2	48.67	7.433	7.562
SC05	270.28	3.652	34.43	−4.33	3	3	2	48.67	8.157	8.416

MW: molecular weight, MS: molecular solubility, MV: molecular volume; the units of energy: Joule; NRB: number of rotatable bonds, NR: number of rings; NAR: number of aromatic rings, NHA: number of hydrogen bond acceptors; NHD: number of hydrogen bond donors, PSA: polar surface area; predicted activity is  $\text{pIC}_{50}$ .

#### 2.4. Ligand de novo evolution

The component with the highest docking score was selected to produce derivatives by the protocol of *de novo evolution*. This drug design program could change the side groups of an assigned molecule based on its build-in library, which could modify the target components to optimize the binding affinity to PDE5. The results of *de novo evolution* were used to confirm the accuracy of docking scores.

#### 2.5. Pharmacophore analysis

The pharmacophore/interaction generation, common feature pharmacophore generation, and ligand pharmacophore mapping on Accelrys Discovery studio V2.1 were employed for simulation interaction between target inhibitors and PDE5. The amino acids around the binding site were analyzed based on three features, hydrogen bond donors, hydrogen bond acceptors, and hydrophobic forces. The calculated results are presented in interaction maps.

### 3. Results

#### 3.1. MLR analysis

Our reliable MLR modeling for the molecule has been published [29]. The molecular properties from Xia's study were incorporated into the QSAR model by the following equation with MLRTemp-

Model values [29]:

$$\begin{aligned}
 [\text{MLRTempModel}] = & -3.259 - 5.359[\text{Molecular.Weight}] \\
 & - 0.9236[\text{A log P}] + 6.434[\text{Energy}] \\
 & - 3.959[\text{Molecular.Solubility}] \\
 & + 5.149[\text{Num.Rings}] \\
 & + 8.689[\text{Num.H.Acceptors}] \\
 & - 4.693[\text{Num.AromaticRings}] \\
 & - 0.415[\text{Molecular.PolarSurfaceArea}] \quad (2)
 \end{aligned}$$

The pharmaceutical activities correlate very well with MLRTemp-Model values ( $R^2 = 0.8484$ ) in this QSAR model [29]. This correlation was used to predict  $\text{pIC}_{50}$  of the major compounds from ESs, CMs, and SCs as shown in Table 4. The predicted activities ( $\text{pIC}_{50}$ ) of ES03b (10.031), CM01 (25.249), CM05 (17.731), SC01 (14.298), and SC03 (11.421) are all significantly higher than that of sildenafil citrate (7.989). In Eq. (2), the number of hydrogen bond acceptors (Num\_H\_Acceptors) has the highest weight of 8.689. Sequentially, the pharmacophore analysis focused on the feature of hydrogen bond acceptors (Fig. 2).

#### 3.2. Virtual screening for docking

The scoring functions of the training set are listed in Table 5; the interaction map of the binding site in PDE-5 is shown in Fig. 2(a).

**Table 5**

The docking results of PDE5.

Name	DS	LigS1	LigS2	−PLP1	−PLP2	−PMF
cGMP	55.67	4.51	5.69	79.95	75.79	65.88
Tadalafil	53.271	2.31	5.35	88.24	78.53	101.9
Sildenafil citrate	64.055	5.51	6.94	108.72	110.4	122.45
ES02	57.864	7.18	7.42	135.02	132.62	184.65
ES03a	64.26	7.17	8.06	165.41	156.11	176.44
ES03b	76.915	8.18	8.02	141.15	131.44	168.93
CM01	41.998	3.65	5.1	65.69	65.49	96.65
CM02	47.294	3.81	5.26	70.13	68.58	104.1
CM03	41.6	3.17	4.77	59.9	56.47	91.71
CM04	51.311	3.25	5.36	79.68	75.43	125.85
CM05	46.703	3.21	5.21	70.48	66.74	120.86
SC01	69.838	6.64	7.25	128.99	129.53	138.22
SC02	43.528	6.45	7.07	97.92	94.66	154.06
SC03	66.433	7	7.31	118.33	113.23	161.2
SC04	52.061	5.67	6.12	77.35	82.42	148.02
SC05	50.497	4.6	5.58	69.6	72.63	136.55



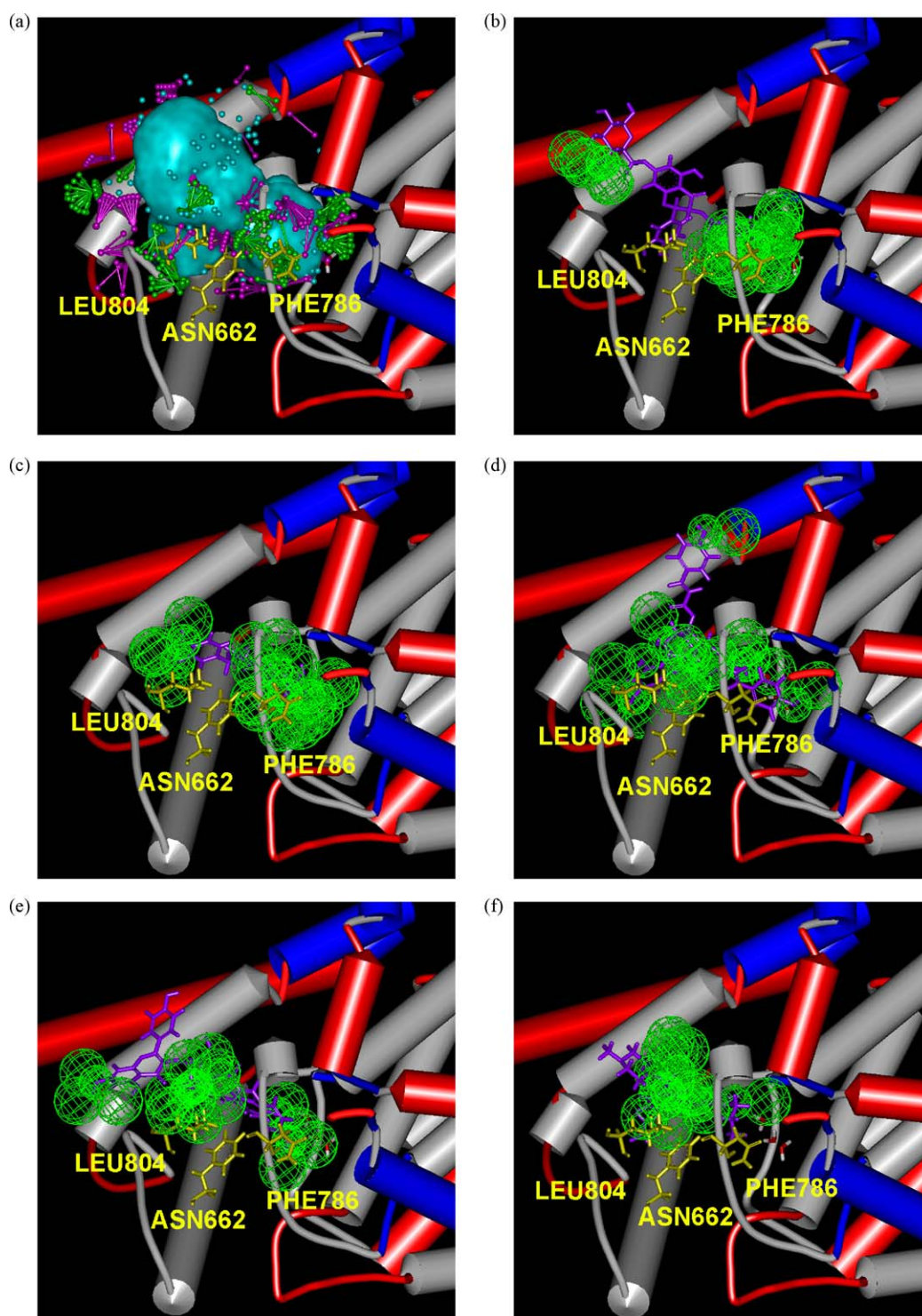


**Fig. 2.** (a) The pharmacophore features of PDE5 around the binding site. The green balls labeled the region of hydrogen bond acceptor. The purple balls labeled the regions of hydrogen bond donor. The blue balls labeled the hydrophobic regions. The pharmacophore features of CS01 (b), CS03 (c), ES03a (d), ES03b (e), and cGMP (f).

The docking scores of ES03b, SC01, and SC03 were 76.915, 69.838, and 66.433, respectively. In control group, sildenafil citrate owns the highest docking score, 64.055. However, it is still lower than that of ES03b, SC01, and SC03. Additionally, ES03b, SC01, and SC03 also show higher predicted activities than those in the control group in the MLR model. Sequentially, ES03b, SC01, and SC03 were employed to *de novo evolution*. The interactions of ligand–protein complex are shown in Figs. 2 and 3. The binding site for PDE5

inhibitors is surrounded by hydrophobic features (Fig. 2(a)), therefore, the designed drugs should have same characteristics, such as aromatic rings in their scaffolds; otherwise, the complex could not form a stable ligand–protein complex. According to Eq. (2), the feature of hydrogen bond acceptors appears to play an important role in the complex formation. Fig. 2(b)–(f) shows the distribution of hydrogen bond acceptors on the PDE5 and four compounds with optimal distribution of hydrogen bond acceptors.

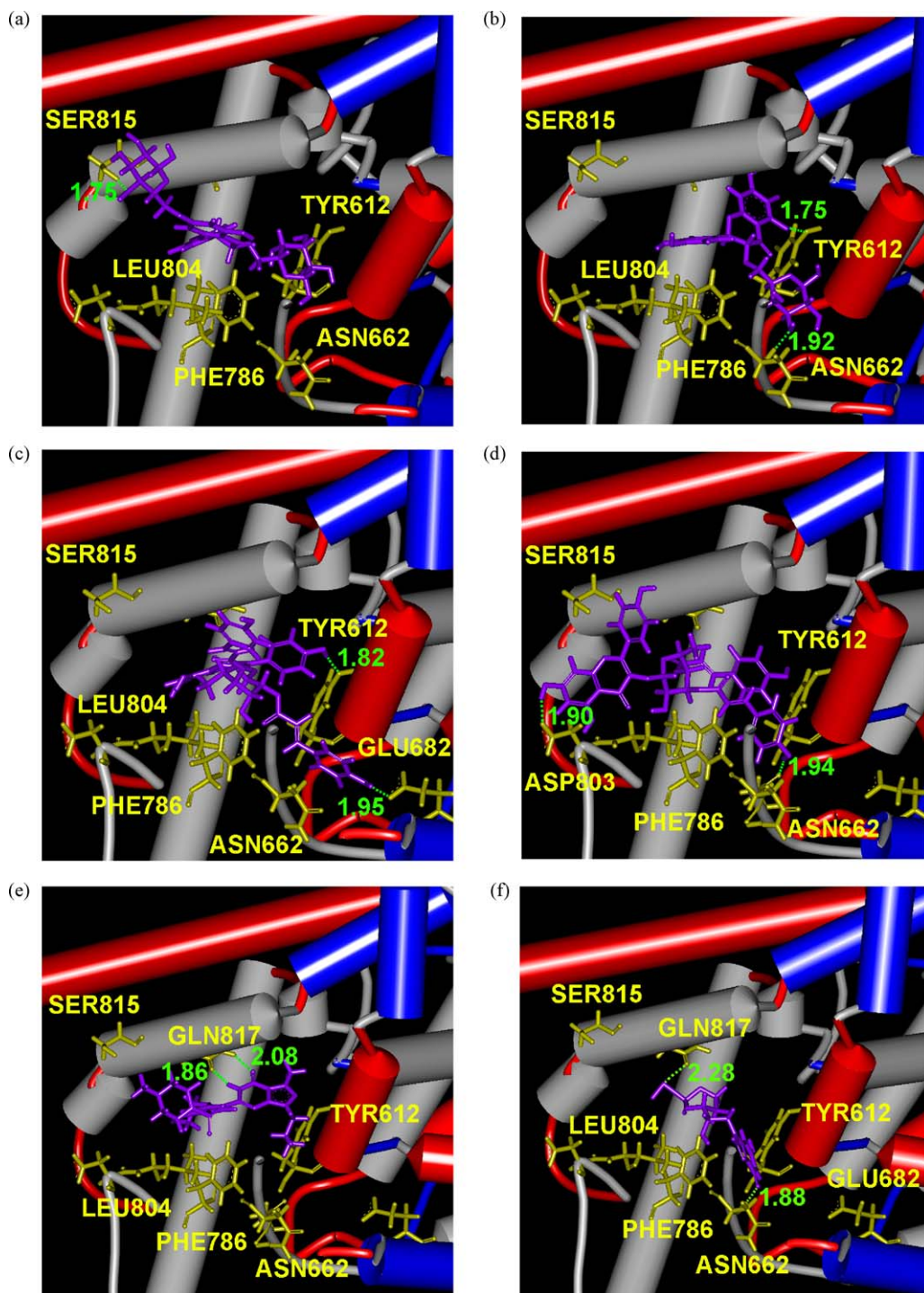


Fig. 3. The docking poses of SC01 (a), SC03 (b), ES03a(c), ES03b (d), sildenafil citrate (e), and cGMP (f).

As seen in Fig. 2(e), the feature of hydrogen bond acceptors of ES03b perfectly matches the PDE5's pharmacophore features on the binding site, in agreement with the finding that ES03b has the highest docking score.

### 3.3. Ligand de novo evolution and scoring function analysis

The molecular structures of *de novo* evolution were showed in Figs. S1–S3. The *de novo* evolution compounds were docked into PDE-5 and calculated by scoring functions. Ligscore 1 and

Ligscore 2 were calculated by the descriptors of polar surfaces of receptor–ligand complexes that are the target compound–PDE5 complexes in this study. As shown in Table 5, no significant difference in Ligscore 1 and Ligscore 2 was noted between the molecules of training set. Compared with the data shown in Tables 5 and 6, Ligscore 1 and Ligscore 2 of herbal compounds in the *de novo* evolution results are indeed higher than those in the control group. The Evo series of compounds are thought to offer more polar interaction areas than cGMP. In fact, the polar surfaces are essential elements in Eq. (2). Piecewise linear

**Table 6**The docking results of the derivatives from *de novo* evolution.

Name		DS	LigS1	LigS2	-PLP1	-PLP2	-PMF
SC01	Evo_4	87.47	7.31	7.49	136.25	139.71	137.79
	Evo_6	85.44	7.2	7.38	132.87	135.96	137.46
	Evo_17	79.48	6.87	6.96	115.47	113.7	142.81
	Evo_26	79.48	6.87	6.96	115.47	113.7	142.81
	Evo_33	76.69	6.37	7.48	128.48	120.55	162.45
	Evo_14	75.06	4.83	6.52	109.48	104.2	129.13
	Evo_23	75.06	4.83	6.52	109.48	104.2	129.13
	Evo_15	72.49	5.94	6.98	117.01	111.96	140.81
	Evo_24	72.49	5.94	6.98	117.01	111.96	140.81
	Evo_29	69.07	6.5	7.74	126.79	117.71	173.73
SC03	Evo_1	88.05	8.22	8.77	144	139.18	204.06
	Evo_12	75.75	6.07	6.55	122.01	123.81	114.18
	Evo_3	74.72	8.29	8.43	137.13	129.61	182.27
	Evo_4	70.68	6.87	7.29	107.08	101.96	205.58
	Evo_11	69.64	5.82	6.22	110.85	115.12	107.13
	Evo_26	69.06	6.69	6.89	117.15	118.93	126
	Evo_7	66.28	7.13	7.38	108.16	99.39	180.79
	Evo_20	66.25	7.08	7.94	141.19	143.26	143.57
	Evo_27	64.20	6.27	6.93	119.3	108.67	162.96
	Evo_2	63.84	7.54	8.21	142.39	134.17	165.93
ES03b	Evo_48	114.461	7.99	7.68	144.31	135.63	180.12
	Evo_45	113.536	7.94	7.51	141.53	132.98	173.2
	Evo_47	113.39	7.99	7.87	144.43	133.86	179.68
	Evo_49	111.962	7.9	7.5	143.14	134.83	174.45
	Evo_36	111.53	7.75	7.51	144.96	138.06	171.5
	Evo_42	109.825	7.89	7.5	139.58	131.11	168.46
	Evo_41	109.581	8.2	7.74	144.61	134.78	173.7
	Evo_25	109.045	8.36	7.45	160.15	154.69	177.54
	Evo_35	108.98	8.37	7.82	161.39	152.67	185.71
	Evo_44	108.429	7.73	7.47	143.62	133.43	178.97
	Evo_39	108.11	8.07	7.58	158.57	149.73	181.25
	Evo_16	106.79	8.05	7.53	143.19	143	179.02
	Evo_24	106.351	8.09	7.58	159.88	149.57	185.43
	Evo_28	103.493	7.97	7.51	152.88	145.81	179.35
	Evo_6	89.923	8.25	7.58	157.98	154.04	193.52
	Evo_15	88.842	8.12	7.94	156.22	145.27	184.05
	Evo_17	88.826	8.05	7.86	159.73	150.9	180.08
	Evo_10	87.701	8.02	7.64	157.63	149.94	174.42
	Evo_22	86.105	7.94	7.64	158.68	150.45	176
	Evo_4	84.983	7.96	7.65	155.06	146.11	173.03
	Evo_9	84.031	7.89	7.7	159.77	150.27	179.7
	Evo_38	83.302	7.82	7.57	144.42	135.3	193.83
	Evo_12	81.758	7.86	7.51	151.48	143	170.99

potential (PLP) scores were calculated based on hydrogen bond formation. High PLP scores indicate strong receptor–ligand binding. The hydrogen bond distribution of target compound–PDE5 complexes is shown in Fig. 3. The PLP scores of Evo series are higher than that of the control groups. Potential of mean force (PMF) scores were calculated by summation of pairwise interaction terms of all interatomic pairs in the receptor–ligand complex. Increased PMF scores are important in cGMP competition with PDE5 inhibitors (Tables 5 and 6). According to PMF scores and docking scores, SC01-Evo4, SC03-Evo1, and ES03b-Evo48 were subjected to pharmacophore analysis. Hydrophobic interaction, entropy, degree of freedom, and energy change were confirmed by Jain, Lig internal energy (LIE), Ludi scores, and binding energy in order to ensure the binding stability in receptor–ligand complex of Evo series were higher than the control groups.

#### 4. Discussion

The center of inhibitor binding site on PDE5 is filled with hydrophobic features (Fig. 2(a)), suggesting that hydrophobic scaffolds could improve the stability of inhibitor–PDE-5 com-

plex. Additionally, Eq. (2) also shows that AlogP and molecular solubility are important elements for MLR analysis. Fig. 2(a) also shows the inhibitor binding site on PDE-5 is twisted by three amino acids: ASN662, PHE786, and LEU804, which cause the detoured ligands (Fig. 2(b)–(f)). Moreover, Eq. (2) indicates the number of “rings” and “aromatic rings” carry weights in compound binding as well. Thus, a suitable amount of ring groups should be considered to add to the scaffolds or side chain of compounds. And a long scaffold may fit the inhibitor binding site on PDE5 as well as a short scaffold. The results of docking scores are in accord with those derived from the MLR analysis. The docking poses of SC01, SC03, ES03a, ES03b, sildenafil citrate, and cGMP are shown in Fig. 3. It is clear that SC01 and ES03b can fully fill in the binding site on PDE-5 but sildenafil citrate and cGMP only occupy the center of the binding site. These data show the design of ligands may be improved by fulfilling the maximum of binding interaction. By *de novo* evolution results (Fig. 4 and Table 6), the docking scores of SC01-Evo4, SC03-Evo1, and ES03b-Evo48 are higher than SC01, SC03, and ES03b, respectively (Tables 5 and 6). This finding indicates that the excellent derivatives from *de novo* evolution are consistent with our MLR and pharmacophore analysis.



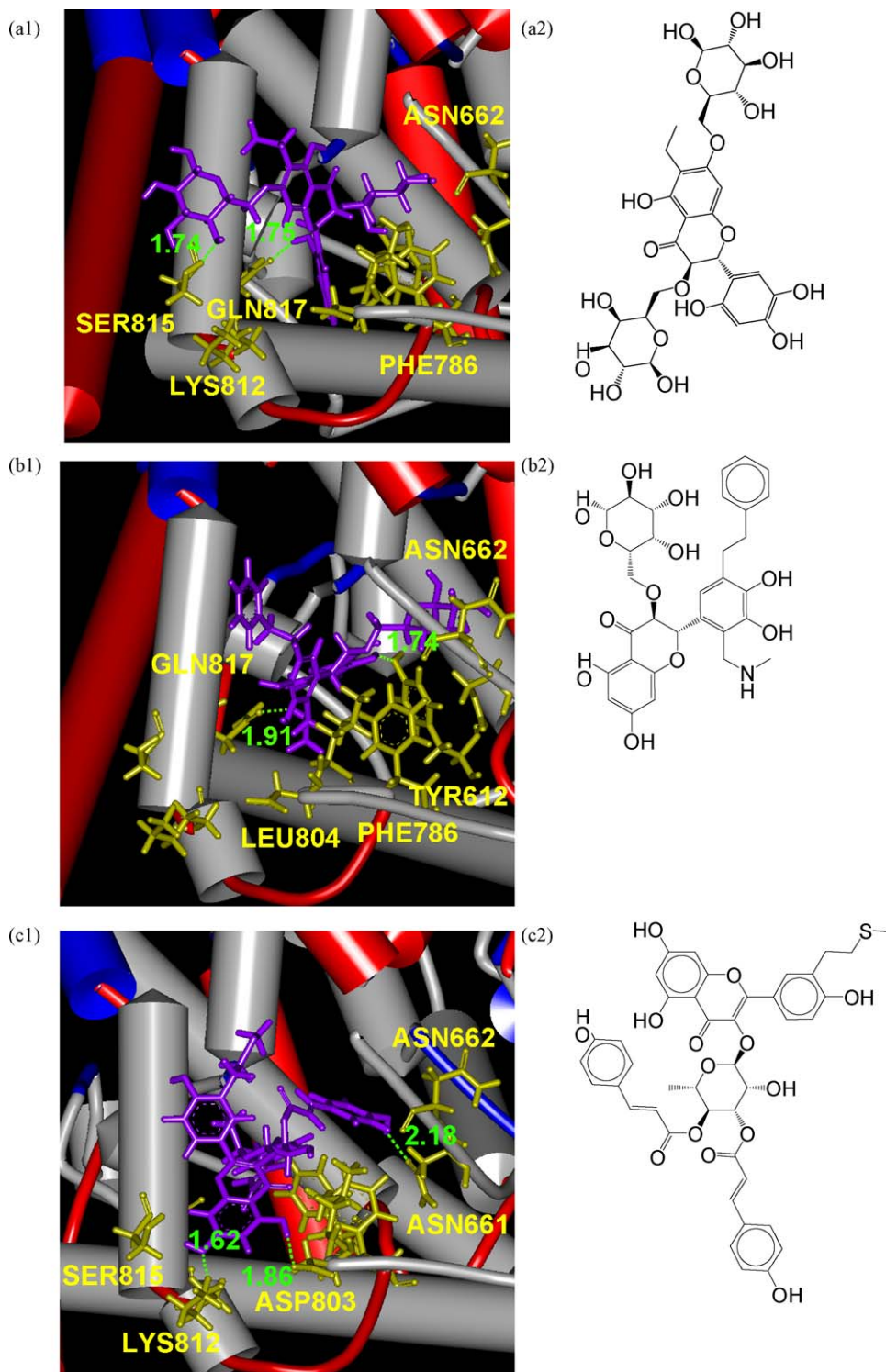


**Fig. 4.** The docking poses of SC01-Evo04 (a1), SC03-Evo01 (b1), and ES03b-Evo48 (c1). The structures of SC01-Evo04 (a2), SC03-Evo01 (b2), and ES03b-Evo48 (c2).

## 5. Conclusion

ESs, CMs, and SCs are well known TCM for treating erectile dysfunction since ancient Chinese era with molecular mechanism of actions remain to be elucidated. The major compounds of these three herbs interact with PDE-5 based on our investigation of ligand–protein interaction. From

Eq. (2) and docking study, we draw the following conclusions:

- (1) The molecular solubility of inhibitors should be hydrophobic in order to fit the core in the PDE-5 binding site.
- (2) The binding site on PDE-5 may have more space for bulky ligands with molecular weights over 500.



- (3) The features of hydrogen bond acceptors, may play an important role in the complex formation,
- (4) According to MLR analysis, the number of ring groups could be up to 6, but the optimum number of aromatic rings was limited to 4 to be potent.

Moreover, the prices of ESs, CMs, and SCs are not expensive, therefore, the extracts of these potential herbs could offer a cheaper way for treating erectile dysfunction. The costs on drug production and synthesis could be significantly decreased based on this study.

### Acknowledgements

The research was supported by grants from the National Science Council of China (NSC 98-2221-E-039-007) and China Medical University (CMU 97-CMC-014, CMU97-276). I am grateful to the National Center for High-performance Computing for computer time and facilities and professional suggestion by Drs. Chung Y. Hsu of China Medical University.

### Appendix A. Supplementary data

Supplementary data associated with this article can be found, in the online version, at doi:10.1016/j.jmgm.2009.08.004.

### References

- [1] R.S. Li, J.L. Li, J.J. Xu, Stimulatory action of epimedium sagittatum (sieb. Et zucc.) maxim. On platelet aggregation in rats, *Zhong Yao Tong Bao* 12 (1987) 40–42.
- [2] K. Feng, W. Xie, B.L. Chen, J.Z. Wang, J.G. Guo, Effect of five species of epimedium on growth of cartilage and proliferation of cartilage cell in vitro, *Zhongguo Zhong Yao Za Zhi* 31 (2006) 2065–2067.
- [3] R. Liu, L. Feng, A. Sun, L. Kong, Preparative isolation and purification of coumarins from *Cnidium monnieri* (L.) Cusson by high-speed counter-current chromatography, *J. Chromatogr. A* 1055 (2004) 71–76.
- [4] M. Ye, Y. Li, Y. Yan, H. Liu, X. Ji, Determination of flavonoids in *Semen cuscuteae* by RP-HPLC, *J. Pharm. Biomed. Anal.* 28 (2002) 621–628.
- [5] J.D. Corbin, S.H. Francis, Cyclic GMP phosphodiesterase-5: target of sildenafil, *J. Biol. Chem.* 274 (1999) 29–32.
- [6] H.H. Yoo, N.S. Kim, G.J. Im, D.H. Kim, Pharmacokinetics and tissue distribution of a novel PDE-5 inhibitor, SK-3530, in rats, *Acta Pharmacol. Sin.* 28 (2007) 1247–1253.
- [7] D. Whitehill, Viagra, levitra, and cialis: what's the difference? *S. D. J. Med.* 58 (2005) 129–130.
- [8] J.L. Weeks, R. Zoraghi, A. Beasley, K.R. Sekhar, S.H. Francis, J.D. Corbin, High biochemical selectivity of tadalafil, sildenafil and vardenafil for human phosphodiesterase 5a1 (PDE-5) over pde11a4 suggests the absence of pde11a4 cross-reaction in patients, *Int. J. Impot. Res.* 17 (2005) 5–9.
- [9] K. Loughney, J. Taylor, V.A. Florio, 3',5'-cyclic nucleotide phosphodiesterase 11a: localization in human tissues, *Int. J. Impot. Res.* 17 (2005) 320–325.
- [10] J.L. Weeks, M.A. Blount, A. Beasley, R. Zoraghi, M.K. Thomas, K.R. Sekhar, J.D. Corbin, S.H. Francis, Radiolabeled ligand binding to the catalytic or allosteric sites of PDE-5 and pde11, *Methods Mol. Biol.* 307 (2005) 239–262.
- [11] C.Y.C. Chen, A novel perspective on designing the inhibitor of HER2 receptor, *J. Chin. Inst. Chem. Engrs.* 39 (2008) 291–299.
- [12] Y.C. Chen, K.T. Chen, Novel selective inhibitors of hydroxyxanthone derivatives for human cyclooxygenase-2, *Acta. Pharmacol. Sin.* 28 (2007) 2027–2032.
- [13] C.Y.C. Chen, Insights into the suanzaoren mechanism – from constructing the 3D structure of GABA-A receptor to its binding interaction analysis, *J. Chin. Inst. Chem. Engrs.* 39 (2008) 663–671.
- [14] C.Y.C. Chen, Discovery of novel inhibitors for c-Met by virtual screening and pharmacophore analysis, *J. Chin. Inst. Chem. Engrs.* 39 (2008) 617–624.
- [15] C.Y. Chen, Y.H. Chang, D.T. Bau, H.J. Huang, F.J. Tsai, C.H. Tsai, C.Y.C. Chian, Ligand-based dual target drug design for H1N1: swine flu – a preliminary first study, *J. Biomol. Struct. Dyn.* 27 (2009) 171–178.
- [16] C.Y. Chen, H.J. Huang, F.J. Tsai, C.Y.C. Chen, Drug design for Influenza A virus subtype H1N1, *J. Chin. Inst. Chem. Engrs.*, (2009), doi:10.1016/j.jtice.2009.06.007.
- [17] C.Y.C. Chen, Pharmacoinformatics approach for mPGES-1 in anti-inflammation by 3D-QSAR pharmacophore mapping, *J. Chin. Inst. Chem. Engrs.* 40 (2009) 155–161.
- [18] C.Y.C. Chen, Chemoinformatics and pharmacoinformatics approach for exploring the GABA-A agonist from Chinese herb suanzaoren, *J. Chin. Inst. Chem. Engrs.* 40 (2009) 36–47.
- [19] Y. Fukunishi, H. Nakamura, Prediction of protein–ligand complex structure by docking software guided by other complex structures, *J. Mol. Graph. Model.* 26 (2008) 1030–1033.
- [20] J. Taminiau, G. Thijs, H.D. Winter, Pharaos: pharmacophore alignment and optimization, *J. Mol. Graph. Model.* 27 (2008) 161–169.
- [21] P. Srivani, E. Srinivas, R. Raghu, G.N. Sastry, Molecular modeling studies of pyridopyrimidine derivatives – potential phosphodiesterase 5 inhibitors, *J. Mol. Graph. Model.* 26 (2007) 378–390.
- [22] B.J. Sung, K.Y. Hwang, Y.H. Jeon, J.I. Lee, Y.S. Heo, J.H. Kim, J. Moon, J.M. Yoon, Y.L. Hyun, E. Kim, S.J. Eum, S.Y. Park, J.O. Lee, T.G. Lee, S. Ro, J.M. Cho, Structure of the catalytic domain of human phosphodiesterase 5 with bound drug molecules, *Nature* 425 (2003) 98–102.
- [23] B.R. Brooks, R.E. Bruccoleri, B.D. Olafson, D.J. States, S. Swaminathan, M. Karplus, CHARMM: a program for macromolecular energy minimization and dynamics calculations, *J. Comp. Chem.* 4 (1983) 187–217.
- [24] G. Xia, J. Li, A. Peng, S. Lai, S. Zhang, J. Shen, Z. Liu, X. Chena, R. Ji, Synthesis and phosphodiesterase 5 inhibitory activity of novel pyrido [1,2-e] purin-4(3H)-one derivatives, *Bioorg. Med. Chem. Lett.* 15 (2005) 2790–2794.
- [25] R. Ghavami, A. Najafi, M. Sajadi, F. Djannaty, Genetic algorithm as a variable selection procedure for the simulation of <sup>13</sup>C nuclear magnetic resonance spectra of flavonoid derivatives using multiple linear regression, *J. Mol. Graph. Model.* 27 (2008) 105–115.
- [26] J.A. Morrill, E.F. Byrd, Development of quantitative structure–property relationships for predictive modeling and design of energetic materials, *J. Mol. Graph. Model.* 27 (2008) 349–355.
- [27] A. Mohajeri, B. Hemmateenejad, A. Mehdipour, R. Miri, Modeling calcium channel antagonistic activity of dihydropyridine derivatives using QTMS indices analyzed by GA-PLS and PC-GA-PLS, *J. Mol. Graph. Model.* 26 (2008) 1057–1065.
- [28] G.B. Fogel, M. Cheung, E. Pittman, D. Hecht, In silico screening against wild-type and mutant Plasmodium falciparum dihydrofolate reductase, *J. Mol. Graph. Model.* 26 (2008) 1145–1152.
- [29] C.Y. Chen, Y.H. Chang, D.T. Bau, H.J. Huang, F.J. Tsai, C.H. Tsai, C.Y.C. Chen, Discovery of potent inhibitors for phosphodiesterase 5 by virtual screening and pharmacophore analysis, *Acta Pharmacol. Sin.* 30 (2009) 1186–1194.